Available online at www.sciencedirect.com
SCIENCE DIRECT®
Cement and Concrete Research 35 (2005) 551–561
CEMENT AND CONCRETE RESEARCH

The use of migrating corrosion inhibitors to repair motorways' concrete structures contaminated by chlorides

Lorenzo Fedrizzi[a,*], Francesca Azzolini[b,1], Pier Luigi Bonora[b,1]

[a]ICMMPM Department, University of Rome "La Sapienza", Italy
[b]Department of Materials Engineering and Industrial Technologies, University of Trento, Trento, Italy

Received 19 September 2003; accepted 10 May 2004

Abstract

The effectiveness of migrating corrosion inhibitors (MCIs) and repair mortars against rebar corrosion was studied in concrete specimens made by ordinary Portland cement with w/c ratio equal to 0.6 and containing 1 wt.% of chlorides. An alkanolamine-based inhibitor was tested in addition with a common mortar and two repair mortars. Electrochemical techniques, measurements of corrosion potential and electrochemical impedance spectroscopy (EIS) were used to determine the corrosion behaviour of the specimens when a cell containing a 3.5% NaCl solution was applied on the rehabilitation mortar. Mercury intrusion porosimetry (MIP) was also used for the characterisation of repair mortars' total porosity and a chemical analysis was made to determine the amount of chlorides penetrated in the mortar layers and in the concrete substrate. Results demonstrate that the simultaneous use of the alkanolamine-based inhibitor with a good barrier coating offers protection against rebar corrosion and allows rehabilitation of deteriorated concrete structures.

Keywords: Corrosion; Concrete; Migrating corrosion inhibitor; Mortars; Chlorides

1. Introduction

Corrosion of reinforced concrete structures is a major problem throughout the world, demanding significant amounts for repair and rehabilitation [1]. Steel in concrete is normally protected from corrosion by the passive film formed at the steel–concrete interface in an alkaline cementitious matrix. However, depassivation can occur either when the pH of the pore solution drops to low values due to carbonatation, or when chloride ions (from deicing salts or from seawater) have penetrated to the reinforcement in sufficient quantities to destroy the protective oxide layer. Corrosion in the form of rust formation and/or loss in cross-section of the rebars will then start in the presence of oxygen and water [2].

One of the main causes of deterioration for motorways' concrete structures built in mountainous areas is just the penetration of chlorides from deicing salts used during the winter season. For a corrosion risk situation or beginning corrosion, preventive measures may be applied; whereas, in severely corroding structures, repairs have to be performed.

Coatings applied to the concrete surface offer an effective and reliable solution for the protection of concrete and the embedded reinforcing steel, either for new construction or for rehabilitation of deteriorated concrete. A protective surface coating demands good adhesion on the concrete, high durability, UV and weather resistance, prevention of water ingress, high resistance against carbon dioxide diffusion, low chloride permeability but water vapour permeability [1].

The repair of damaged reinforced concrete structures can be made using a new range of ready-mixed mortars [3]. These materials may consist of polymer-modified mortars or may be prepared using different kinds of additives, such as silica fume or fly ashes. Migrating corrosion inhibitors (MCIs) can also be added.

Chemical corrosion inhibitors are an alternative, cost-effective method to prevent and delay the onset of

* Corresponding author. Department of Materials Engineering and Industrial Technologies, University, Mesiano di Povo, Trent 38050, Italy. Tel.: +39-461-882425; fax: +39-461-881977.
E-mail addresses: Lorenzo.Fedrizzi@ing.unitn.it (L. Fedrizzi), francescaazzolini@yahoo.it (F. Azzolini), Pierluigi.Bonora@ing.unitn.it (P.L. Bonora).
[1] Fax: +39-461-881977.

0008-8846/$ – see front matter © 2004 Elsevier Ltd. All rights reserved.
doi:10.1016/j.cemconres.2004.05.018

corrosion or to reduce the corrosion attack of reinforcement in concrete [4]. These substances can be added as admixtures to concrete/mortar or can be directly applied on the concrete surface. Any inhibitor should have good solubility characteristics in the concrete and rapidly reach the metal corroding surface. In addition, the physical and durability properties of concrete should not be adversely affected.

Many substances have been tested as inhibitors against the corrosion of reinforcing steel bars, e.g., calcium nitrite, sodium monofluorophosphate and alkanolamines. Alkanolamine-based corrosion inhibitors are classified as MCIs, because they can move via diffusion through the pore structure of concrete to reach the surface of steel bars [1]. Upon contact with reinforcing steel, inhibitor's molecules form a monomolecular protective layer which reduces corrosion by protecting the anodic as well as the cathodic areas of the rebars [3]. They are referred as mixed inhibitors, because they influence both the cathodic and anodic processes of corrosion.

Contradictory results have been recently reported in investigations testing MCIs. Elsener et al. [5] reported low efficiencies of these substances in protection levels. On reinforced mortar samples showing chloride-induced pitting corrosion, no reduction of the corrosion rate could be detected after inhibitor surface application. Bavarian and Reiner [6] found that MCI products offer protection for the steel rebar in aggressive environments by suppressing the chloride ions.

In the present study, the efficiency of the repair mortars' barrier effect and of the MCI has been tested using corrosion potential (E_{corr}) versus time measurements, electrochemical impedance spectroscopy (EIS) and, at the end of the monitoring period (from 220 to 420 days), chloride penetration analysis.

Mercury intrusion porosimetry (MIP) has also been made on the repair mortars to have a preliminary characterisation of the tested products, because many properties of concrete are directly or indirectly affected by its porosity. Characterisation of concrete's porosity is often of great interest in order to explain differences between, and give insights into, these properties. MIP is a widely used method for studying porous materials, in particular cement-based materials. It provides a function of cumulative pore volume versus applied pressure [7].

2. Experimental

2.1. Materials

The concrete specimens were cast in parallelepiped blocks ($30 \times 30 \times 9$ cm^3) using an ordinary Portland cement (CEM II/B-L32.5R UNI ENV 197-1), aggregates (fine 0–5 mm, coarse 5–8 mm), water (to obtain a water/cement ratio equal to 0.6) and sodium chloride (1% of Cl^- by weight of cement). The mixture proportions are shown in Table 1. Six rust-free steel (FeB44k) rods (∅ 10 mm, 400 mm length) were embedded into the concrete and used as rebars. The rebars were placed at two different depths from the upper surface of the specimen as shown in Fig. 1. The cover depth of concrete was 0 mm for top bars and 15 mm for bottom bars.

The choice of the high w/c ratio was made to obtain a high-porosity concrete that would promote an accelerated life test and simulate the worse condition of a real structure, because on site, the ideal ratio (0.4) is not always obtained. The addition of sodium chloride in the mix water was made to simulate a real rehabilitation condition, where the front of chlorides has achieved the rebars in sufficient quantities to break down the passive layer.

At the end of the curing period (at least 28 days), the superior surface of each specimen was coated with one of three different types of mortar of 1 cm thickness, with or without the previous addition of an MCI at the interface between the concrete substrate and the coating. A quantity from 60 to 70 g per specimen of the alkanolamine-based inhibitor was applied by brush on the surface of the concrete before applying the repair mortars, according to the instructions given by the manufacturer. The trade name of the product is Tecnochem MuCis mia 200.

A mortar based on Standard Sand and two different kinds of repair mortars were used as coatings.

The first type of coating (Standard Mortar) was prepared to have a reference specimen for the evaluation of the anticorrosion repair mortars' efficacy and to study the action of the MCI. It was based on Standard Sand (ISO 679 EN 196-1).

The second type of coating (Mortar type A) was a cement mix with w/c ratio equal to 1:6. It contained polyacrylonitrile (PAN) fibres and additives to improve rheological properties but did not hold corrosion inhibitors into the mix. Its trade name is Tecnochem Into BS 37 RS.

The third coating (Mortar type B) was prepared by mixing cement with fine aggregates (0.5 mm) and water with the following sand/cement mix/water ratio: 6:3:1. The cement mix contained MCIs and silica fume. The result of the mix design was a very compact mortar with low porosity. The trade name of the cement compound is Tecnochem MuCis BS 40 M6.

Table 1
Mix design of concrete

Constituents	Quantities
Portland cement	350 kg/m^3
Water	210 l/m^3
Aggregates	1700 kg/m^3
Sand 0–5	850 kg/m^3
Gravel 5–8	850 kg/m^3
NaCl	5.8 kg/m^3

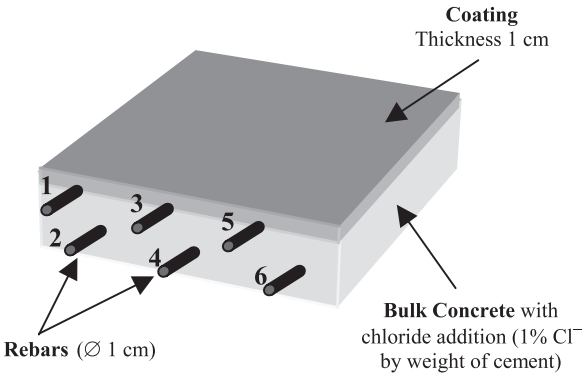

Fig. 1. Geometry of the specimens.

After the mortar curing period (at least 7 days) on the rehabilitation mortar of the specimen, a small plastic cell, open on both sides, was applied.

A solution of 3.5% NaCl by weight of distillate water, which is a typical solution used to test resistance to chlorides attack, was put in the cell, directly in contact with the mortar. The cell with the salt solution was applied to simulate the atmospheric chloride-contaminated water, which is present on the road pavements of the motorway viaducts during the winter season due to the use of deicing salts. The specimens were kept on special supports during all the monitoring time, to allow a free oxygenation also from the bottom side. The exposure conditions are shown in Fig. 2.

2.2. Methods

Each test was made at least in triplicate.

2.2.1. Corrosion potential measurements

During the exposure of the specimens to the corrosive environment, the half-cell potential of the rebars was periodically measured versus the Ag/AgCl reference electrode.

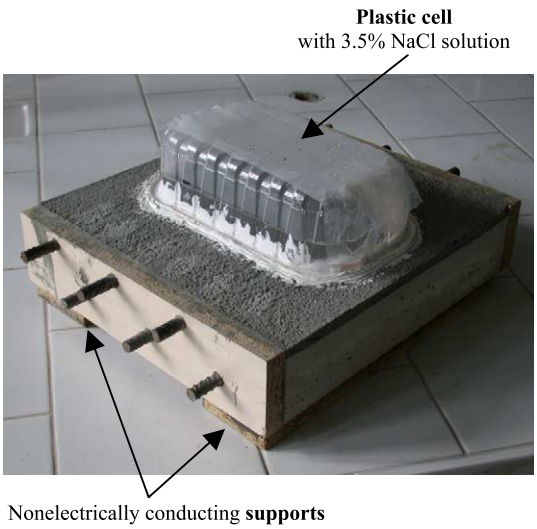

Fig. 2. Exposure conditions.

Working and reference electrode were connected to a potentiostat/galvanostat EG&G 273A, which worked as a high impedance voltmeter. Data obtained for each sample were plotted to show the graphs of potential versus time for upper and lower bars.

2.2.2. EIS measurements

EIS deals with polarising reinforcing steel with a weak alternate current (AC) against a counterelectrode, and with measuring steel potential E, against a reference electrode [8].

The EIS equipment used included an EG&G 273 Potentiostat and a Schlumberger SI 1255 Frequency Analyser, a platinum electrode as counter and an Ag/AgCl electrode as reference. Steel was polarised at $\pm$ 10 mV around its zero-current potential. The frequency range was chosen between 100 kHz and 1 mHz; the maximum limit was imposed by the generator/analyser. The whole experiment was under computer control and a computer interface conveniently stored the impedance data before analysis.

A schematic diagram of the corrosion test setup used for potential and EIS measurements is shown in Fig. 3.

2.2.3. Mercury intrusion porosimetry

MIP is a widely used technique for characterising the distribution of pore size in cement-based materials. It is a simple and quick indirect technique, but it has limitations when applied to materials that have irregular pore geometry [9]. The usual interpretation of such measurements is based on certain assumptions; one of these is that each pore is connected to the sample surface directly or through larger pores, a criterion which is not likely to be met by normal porous materials. Pores not meeting this assumption are called "ink-bottle" pores. Furthermore, the intrusion–extrusion cycle does not close when the initial pressure is reached (hysteresis), indicating that some mercury has been permanently entrapped in the sample pore space [7].

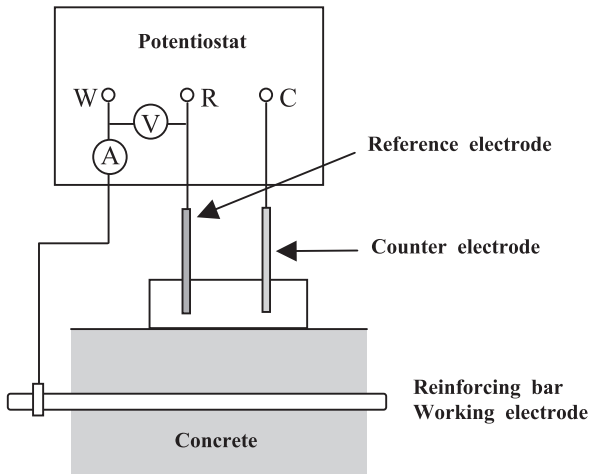

Fig. 3. Schematic diagram of the corrosion test setup (potential and EIS measurements).

With MIP, small porous samples are dried to empty the pores of any existing fluid, introduced into a chamber, which is evacuated and then surrounded by mercury. Pressure in progressive increments is applied to force mercury into the pores of the sample and the intrusion of mercury at each step is monitored [10,11]. The drying procedure involved furnace drying at the temperature of 70 °C until reaching the stabilization of the sample's weight.

By tracking pressures and intrusion volumes during the experiment, it is possible to get a measure of the connecting pore necks of a continuous system or a breakthrough pressure in a discontinuous system. The pore width corresponding to the highest rate of mercury intrusion per change in pressure is known as the "threshold", "critical" or "percolation" pore width. Using this technique, it is also possible to obtain a measure of the total porosity in the sample as that corresponding to the volume of mercury intruded at the maximum experimental pressure divided by the bulk volume of the unintruded sample [10].

The equipment used for porosity measurements was composed by Pascal 140 to determine macroporosity and Porosimeter 2000 to reveal microporosity. The data obtained were automatically combined by a computer program to have the global trend from atmospheric pressure to 200 MPa.

2.2.4. Analysis of penetration of chlorides

A chemical analysis of the chloride penetration at different depths of the repair mortars has been made using the Mohr method [12]. A solution of 0.1 N $AgNO_3$ has been used to titrate and a solution of K_2CrO_4 has been used as indicator. Some mortar powder has been drawn using a drill, and then dissolved in distilled water. The solution has been filtered, acidified with nitric acid to obtain a pH between 6 and 9 and then the indicator was added. The titrating solution was added to the solution drop by drop until the equivalence point was reached, corresponding to the colour change from yellow to red. The amount of chlorides was calculated from the amount of $AgNO_3$ added, using the following relation:

$$1\text{ml } AgNO_3\ 0.1\text{ N} = 3.55\text{ g } Cl^-$$

3. Results

3.1. Mercury intrusion porosimetry

From the MIP volume/pressure intrusion curve, it is possible to extrapolate the mercury total cumulative volume, the total porosity and the pore size distribution. But MIP cannot provide a true pore size distribution, because mercury must pass through the narrowest pores connecting the pore network [10]. Diamond [11] states that MIP measurements are useful to provide threshold diameters and intrudable pore space measurements, which can serve as comparative indices for the connectivity and capacity of the pore systems in hydrated cements, and should be abandoned as measures of the actual pore size present. Anyway, we used MIP measurements to obtain a rough evaluation of the pore size distribution.

The results found during the investigation, summarised in Table 2, show that the Standard Sand mortar is the most porous while better results are obtained testing Mortar type A and especially Mortar type B.

The Standard Mortar has the highest porosity among the considered specimens and a wide range in pore size distribution, from 30 to 30,000 Å (Fig. 4a).

The Mortar type A has the same range in pore size distribution and a total porosity not very different from that of the Standard Mortar. However, this mortar has a very narrow porosity distribution peak and the lowest critical pore width value, centred around 350 Å, as shown in Fig. 4b. This is a very important data, especially because Cook and Hover [10] maintain that the threshold or critical pore width may provide a good indicator of material durability as it has an important influence on the permeability and diffusion characteristics of the cement paste.

The Mortar type B seems the best from the porosity point of view with the lowest mercury cumulative volume, which means the lowest total porosity (Table 2), and with the lowest pore size distribution range, but it has a higher critical pore width value than Mortar type A (around 4000 Å), as shown in Fig. 4c.

3.2. Corrosion potential measurements

Corrosion potentials of the six rebars of each specimen have been measured during the exposure time. An average between the three upper bars and the three lower bars has been made to obtain a statistical value of the potential versus time trend. The results obtained are shown in Fig. 5. The dispersion, however, has been considered for the discussion of the overall trend.

The measurements summarised in Fig. 5 reveal interesting differences from the point of view of the barrier effect offered by the coatings.

The graphs also show the effect of inhibitor treatment on the potential of the reinforcing bars of the specimens, which were subjected to ponding by a sodium chloride solution besides the already present amount of chlorides added in the concrete mix.

Table 2
MIP results: total cumulative volume (measured) and total porosity (calculated) of the repair mortars

Repair mortar	Total cumulative volume (mm^3/g)	Total porosity (%)
Standard mortar	55.78	12.8
Mortar type A	48.84	11.7
Mortar type B	37.02	8.9

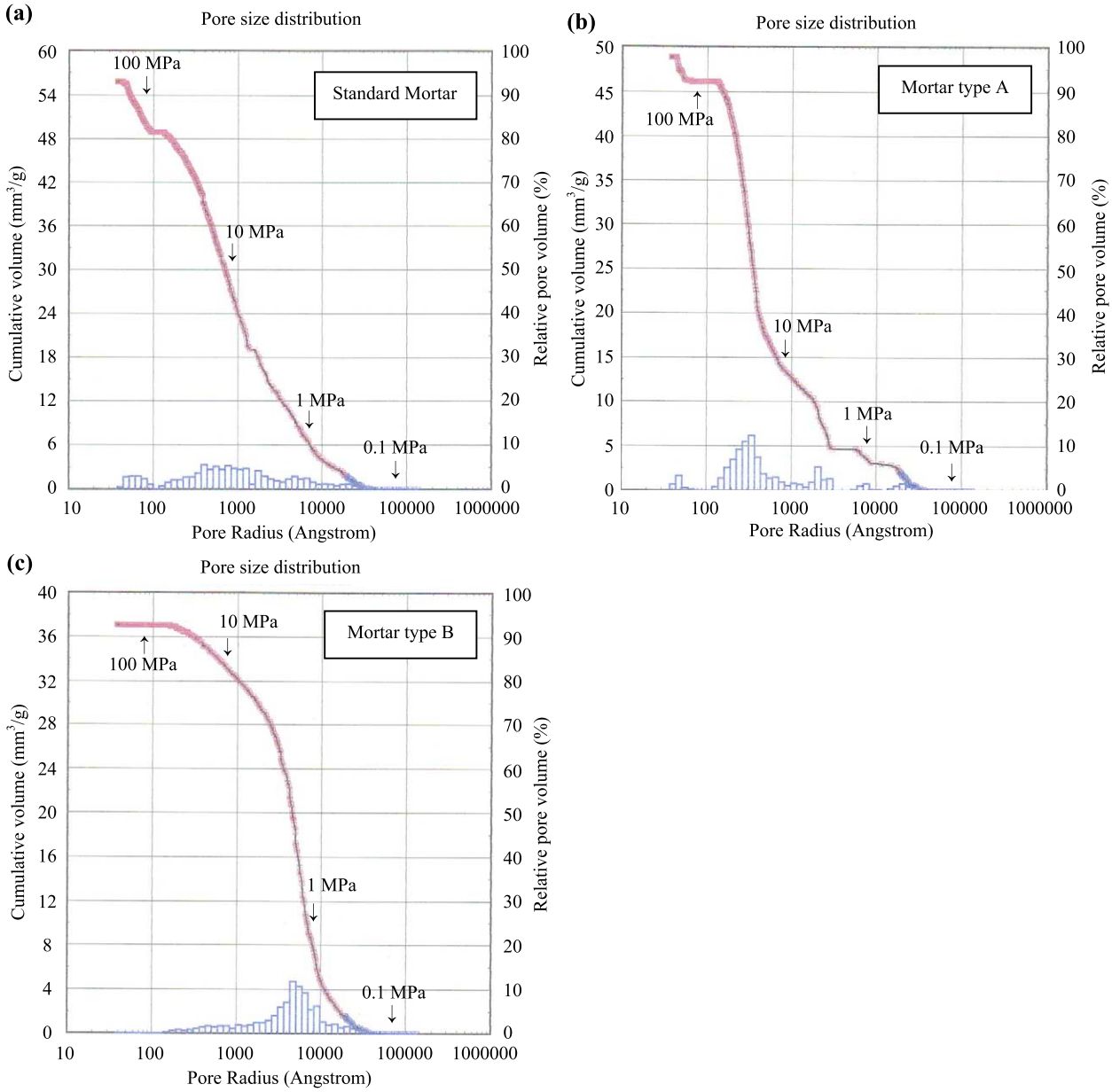

Fig. 4. Each curve represents the total cumulative volume as a function of the applied pressure, from which the relative pore size distribution is obtained as a function of the filled volume. (a) Standard Mortar; (b) Mortar type A; (c) Mortar type B.

The mean potential values of the upper and lower steel bars show that the repair mortars A and B offer a better barrier effect compared to the Standard Mortar of reference (Fig. 5a and c).

With control specimen (covered with Standard Mortar and free from inhibitor), the potential was very and permanently negative, especially for the upper rebars (Fig. 5a). It means that since the beginning of the experimentation, reinforcing steel was depassivated by chloride ions and corrosion occurred. During the first days of exposure, the potential values of the upper rebars start shifting towards more negative potentials. This behaviour could be due to the increase of chloride concentration at the rebar surface coming from the salt solution. But it could also be caused by the higher conductivity of a wetted system.

The potential measurements on the Standard Mortar rebars were stopped after approximately 270 days because the specimens were completely collapsed from a corrosion point of view.

It is interesting to note that the samples with the alkanolamine-based inhibitor applied at the concrete–mortar interface have corrosion potential values (Fig. 5b and d) less negative or similar to those of control specimens, covered with the different coatings but without the MCI (Fig. 5a and c). In particular, the upper rebars have nobler potentials since the beginning (Fig. 5b versus 5a).

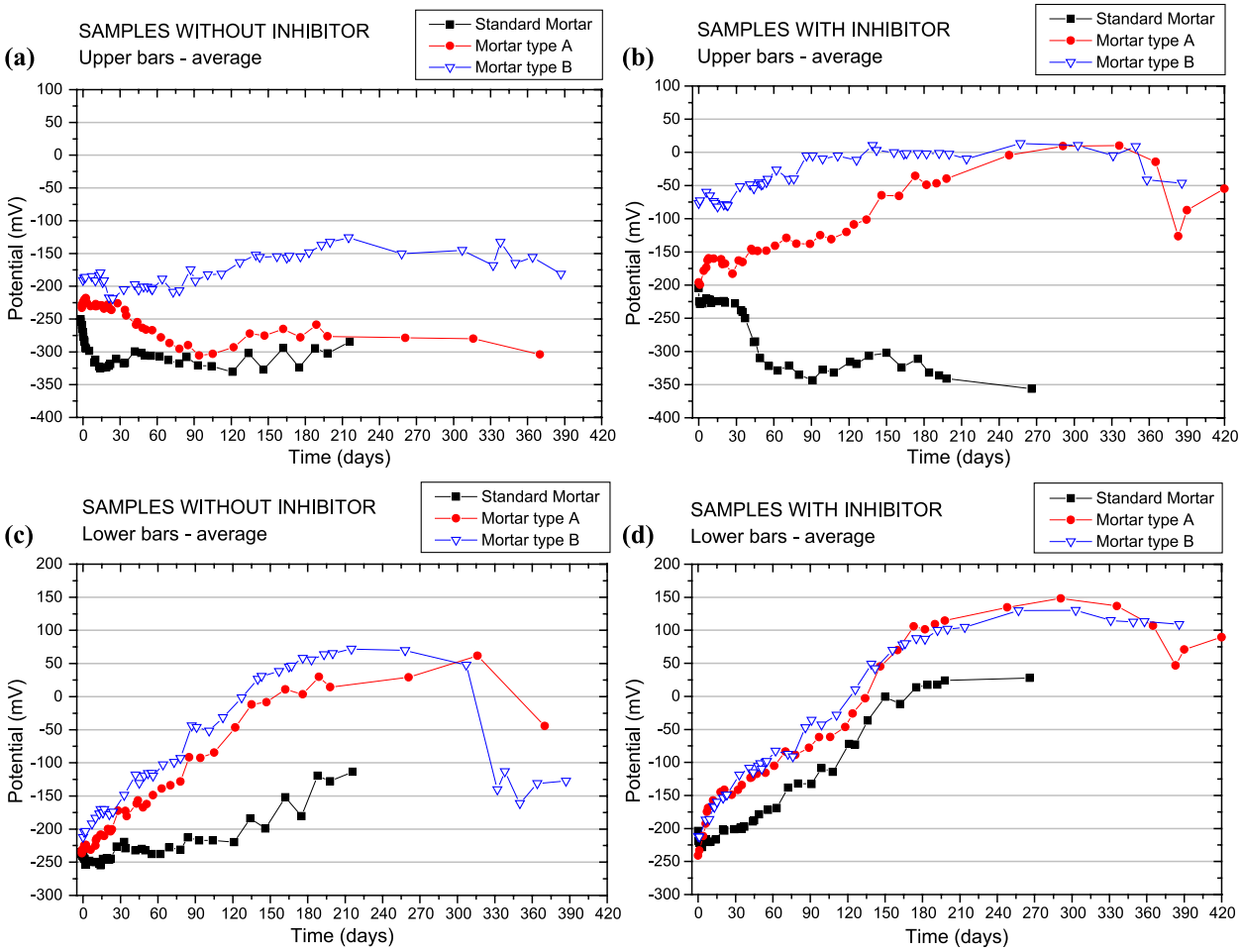

Fig. 5. Corrosion potential (versus Ag/AgCl) versus time diagrams. (a) Blank specimens, average between the three upper bars; (b) Samples treated with the inhibitor, average of the three upper bars; (c and d) Average of the three lower bars of samples without (c) and with (d) the inhibitor added at the concrete–mortar interface.

In the case of the Standard Mortar, the use of the inhibitor only delays the initial collapse of the potential of the upper bars of about 30 days (Fig. 5b versus 5a). On the other hand, when associated to the repair coatings type A and B, the inhibitor can act in the long period with the increase of the potential of all the bars even after 1 year of exposure to the NaCl solution. The rebar corrosion potential values of these treated specimens show an increasing trend in time, reaching values characteristic of passive steel.

From the comparison between the lower rebars of samples treated with the inhibitor and those of untreated samples (Fig. 5d versus 5c), it is possible to note a similar trend in corrosion potential values, even if more noble values are reached by the samples with the inhibitor. In particular, in the case of Standard Mortar with inhibitor, the increase in corrosion potential is clearer than in the specimen without inhibitor and in the case of Mortar type B, there is no collapse at 300 days of exposure as it occurs in the sample without inhibitor.

Moreover, a lower standard deviation of data has been generally obtained for the values measured at the rebars of the specimens treated with the inhibitor.

3.3. EIS measurements

The EIS is a powerful and general technique suitable for characterising the electrochemical processes in inhomogeneous or multiphase materials. It can estimate a steady-state corrosion rate and subsequently, the efficiency of corrosion inhibitors [8].

EIS has been extensively used to try to evaluate the corrosion rate of the steel/concrete system. This technique may be very attractive because, used in a wide range of frequencies, it can give detailed information about the mechanism and kinetics of the electrochemical reactions. Not only it is able to give R_{ct} (R_p) values, related to corrosion rate through the Stearn–Geary formula, but also it may give complementary information on the corrosion process, the dielectric properties of the concrete (high frequency range) or the characteristics of the passivating film (very low frequency) [13].

EIS measurements permit to extrapolate from the fitting of the Nyquist plots the concrete electrical resistance R_0, the charge transfer resistance R_{ct} and the polarization resistance R_p, as shown in Fig. 6. In EIS graphical extrapolation

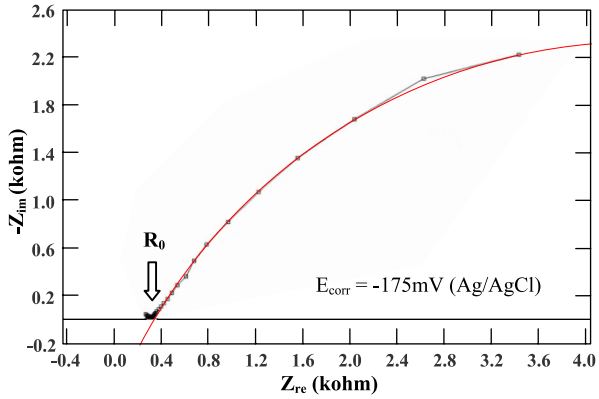

Fig. 6. Example of extrapolation of R_0 and R_{ct} from a Nyquist plot referred to the Standard Mortar sample, rebar n. 2. In particular, the R_{ct} value corresponds to the diameter of the fitted semicircumference.

techniques, the R_0 corresponds to the minimum on the Nyquist diagram at the high frequencies, while R_{ct} is given by the diameter of the fitted semicircle.

The R_0 value is the sum of the electrolyte and the concrete resistance. The resistance of the electrolyte is very low compared with the concrete resistance, due to the high concentration of chlorides in the solution, so it can be neglected. Therefore, R_0 represents the concrete resistance.

From the value of R_0, it is possible to calculate the resistivity of the concrete. In particular, from the R_0 (Ω) values extrapolated from the Nyquist plots referred to the upper bars, it is possible to obtain the resistivity of the mortar ρ_{mortar} (Ω·m) using the following equation:

$$\rho_{mortar} = R_0 \frac{A}{L}$$

where A (m^2) is the wetted area of the rebar, valued about 38×10^{-4} m^2, and L (m) is the thickness of concrete cover, equal to 1×10^{-2} m^2.

As reported by the diagram in Fig. 7, the mortars' resistivities have the tendency to increase in time. It can be explained by the fact that hydrating cement products decrease the porosity of concrete and increase concrete resistivity as referred by Dhouibi et al. [8].

Another important consideration can be deduced from the observation of the graph: the average resistivity of Mortar type A is three time greater than Standard Mortar one and that of Mortar type B is five time more, even if there is a bigger dispersion in the values of resistivity for the mortars that have higher values. The interesting correlation of these results with the porosity values found using MIP will be discussed afterwards.

The value of the corrosion current (I_{corr}) is calculated using the well-known Stearn–Geary equation:

$$I_{corr} = \frac{B}{R_p A}$$

where B is a constant, approximately 26 or 52 mV for active or passive steel embedded in concrete, A (m^2) is the wetted area of the rebar, valued 38×10^{-4} m^2, and the charge transfer resistance (R_{ct}) has been used as R_p (Ω). The value of R_{ct} has been deduced from the steel–concrete system response to the electrical signal applied during impedance measurements.

The corrosion level is considered negligible when I_{corr} is less than 0.1 $\mu A/cm^2$, while it is considered low in the range between 0.1 and 0.5, moderate from 0.5 to 1 and high for values superior to 1 $\mu A/cm^2$ [14].

From the point of view of the corrosion rate, the summary diagrams of Fig. 8 have been obtained. The steel corrosion rates, relevant to three ponding periods, have been reported.

The comparison among the corrosion rates of the upper bars (Fig. 8a) shows that the Standard Mortar alone cannot offer a sufficient barrier action against rebar corrosion in these severe conditions. I_{corr} increases with the exposure time for the upper rebars of the reference specimen, which means high corrosion levels reached, while its average value is low for the deeper reinforcements (Fig. 8c) and has the tendency to decrease in time. A similar trend in upper rebars corrosion rates (Fig. 8a) is evident for Mortar type A, with increasing values of I_{corr} versus time, but delayed 20 days and always at lower values than Standard Mortar. Very different is the behaviour of Mortar type B, whose average upper rebars I_{corr} remains stable and low during the first 200 days.

The addition of the migrating inhibitor shows its effect on Standard Mortar sample in the first days of the monitoring period, delaying the onset of the severe corrosion on the upper rebars (Fig. 8b). There are no significant differences between the lower rebars with or without inhibitor addition (Fig. 8d versus 8c); in both conditions, the tendency is to diminish the corrosion rate.

The comparison between the upper bars (Fig. 8b versus 8a) shows the long-term efficacy of the MCI when associated to repair mortars, such as Mortar type A and Mortar type B. From these data, it would appear that the inhibitor treatment was capable of influencing I_{corr} at both cover depths so that values eventually fell to

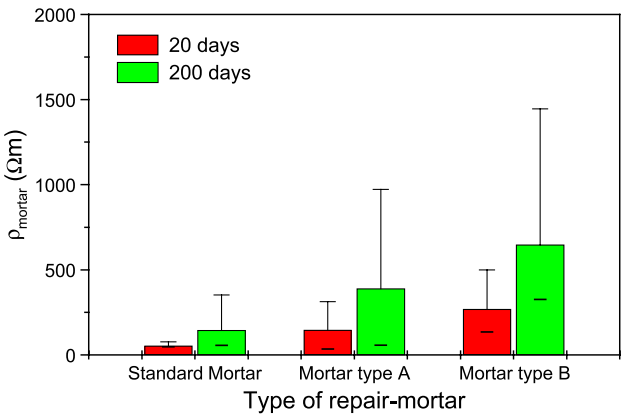

Fig. 7. Average values of R_0 calculated after 20 and 200 days from the beginning of the monitoring.

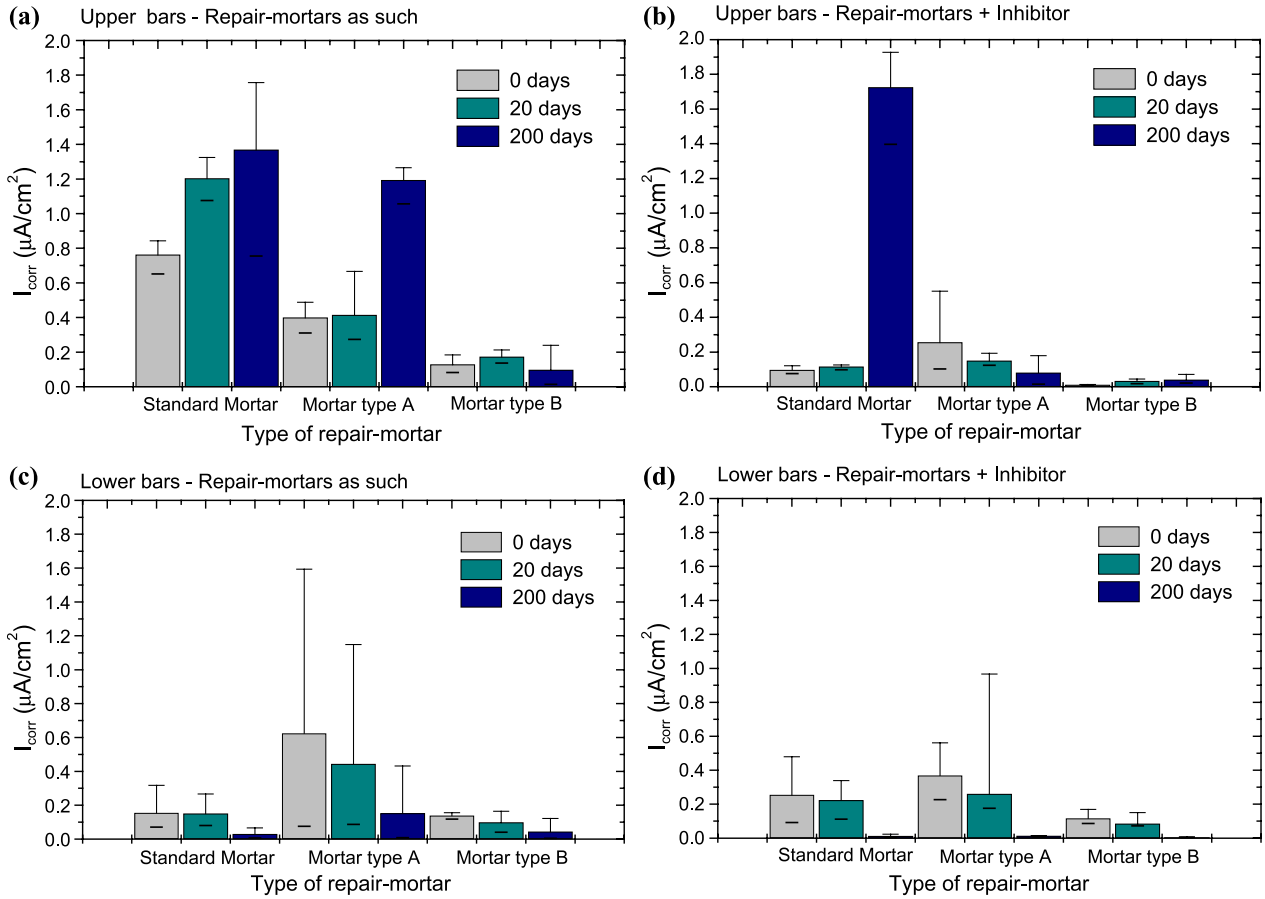

Fig. 8. Corrosion rates (I_{corr}) calculated at three different monitoring periods (beginning of ponding, and after 20 and 200 days) for the upper and lower bars of the specimens. (a and c) Repair made using only the rehabilitation mortar; (b and d) repair made using the rehabilitation mortar and the MCI.

levels typically associated with passivation (<0.1 μA/cm^2). These mortars offer a better protection to the upper bars even when used without inhibitor, especially Mortar type B.

There is a common tendency to repassivation for the lower rebars of all the specimens in both conditions, with or without the inhibitor (Fig. 8d and c). It cannot be stated for sure that the inhibiting effect is visible at the deeper cover depth, even if the corrosion level at 200 days of testing is lower for the samples with the migrating inhibitor.

It is also interesting to consider the general compatibility of data obtained with potential measurements and corrosion rate measurements. The only data that are very different are those related to the lower bars of the specimen covered with Mortar type A, where the I_{corr} values show big dispersions probably associated to some fitting problems of the impedance data.

3.4. Analysis of penetration of chlorides

The chemical analysis of chloride concentration has been made after the removal of the cell with electrolyte, which means at the end of the monitoring period of each specimen.

Fig. 9 presents the chloride concentration profiles obtained from the titration of the mortar/concrete powder extracted at different depths, starting from the top "wetted" area of the upper surface. At least two measures for each depth have been made to test titration reproducibility. It is also reported the chloride level in the bulk concrete, measured on blank concrete powders and corresponding to the initial chloride content included in the concrete casting.

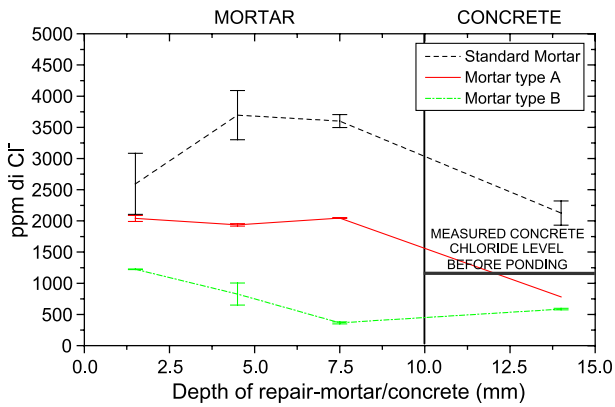

Fig. 9. Measured chloride quantities at different depths of the repair mortars and in the first layer of concrete substrate.

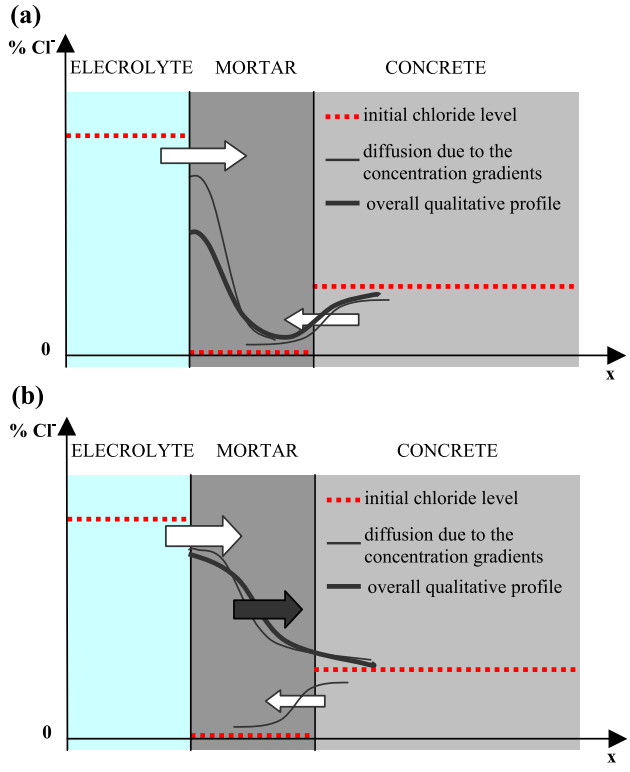

Fig. 10. Schematic representation of the hypothetic chlorides diffusion from electrolyte and contaminated concrete to repair mortar when the repair mortar shows low (a) or high (b) permeability to aggressive substances.

Vaysburd and Emmons [15] say that it is likely that chloride ions from chloride-contaminated existing concrete will move into the repair phase and react with the inhibitor, if present, reducing its critical concentration. In the light of these considerations, it has been supposed that, in addition to the chloride diffusion from electrolyte to the repair mortar due to the gradient of concentration, there was also diffusion from the contaminated concrete to the repair phase.

This hypothesis could explain the chloride concentration profile of the specimen covered with the Mortar type B, which has in the concrete substrate lower values than the initial measured level. This mortar has very low permeability to aggressive substances and a schematic representation of the hypothetical chloride diffusion is shown in Fig. 10a.

The diffusion from concrete to mortar is not evident in high permeability mortars, such as Standard Mortar, due to the dominant diffusion from electrolyte to mortar. The value relative to the concrete layer shows that the chloride ions reached the concrete substrate and the hypothetical diffusion scheme is drawn in Fig. 10b.

An intermediate behaviour between Standard Mortar and Mortar type B was found for the repair-mortar type A. The chloride level in the concrete substrate is low, showing that the mortar offers a good barrier effect to the penetration of chlorides.

The best mortar from the point of view of chloride penetration resistance is Mortar type B, with very low quantities of chlorides in the layers of the mortar and in the first concrete substrate layer. It is interesting to consider that this mortar was the one having the lower porosity and the higher resistivity; these characteristics can explain its high resistance to the penetration of aggressive substances.

During the present investigation, different kinds of laboratory techniques have been used and compared to have the most complete information about the anticorrosion systems analysed and to evaluate the congruence of the various measurement systems.

A first characterisation of the mortars has been made using MIP, while the corrosion progress was monitored in time following the variations of the main electrochemical parameters: the corrosion potential E_{corr}, the electrical resistance R_0 and the charge transfer resistance R_{ct}. The last parameter was used to estimate the rebar corrosion rate I_{corr}. At the end of the monitoring period, the chloride penetration analysis has been carried out.

It has been found out that there is a correspondence between the results of the corrosion potential measurements and the charge transfer resistance measurements, as shown in Fig. 11. This means that the charge transfer resistance

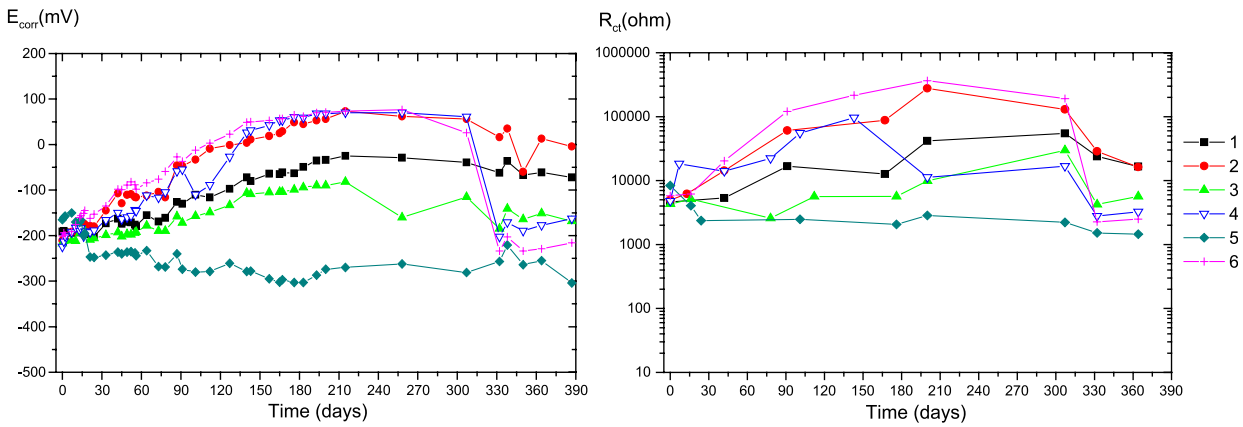

Fig. 11. Mortar type B—comparison between E_{corr} and R_{ct}. 1, 3 and 5 are the upper rebars while 2, 4 and 6 are the lower rebars.

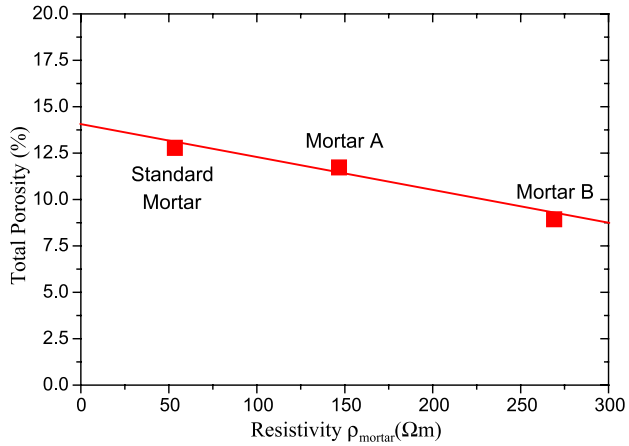

Fig. 12. Comparison between the total porosity obtained with MIP and the average mortar resistivity obtained from the EIS measurements.

values decrease as the corrosion potential changes from passive to active condition. Moreover, the mortar's total porosities, obtained by MIP measurements, gave results inversely proportional to the average mortar's resistivities, calculated from the concrete electrical resistance of the EIS measurements, as demonstrated in Fig. 12. Even the chloride concentrations measured in the different mortars are compatible with the porosity, the electrochemical parameters and the potential measurements.

This gives an idea of the reliability and congruence of the different kind of measurements used during this experimentation.

4. Conclusions

It must be emphasised that no laboratory investigation can fully simulate the performances of concrete repair systems that are used and exposed under different circumstances on real structures. However, to have the most reliable tests, great importance has been given to the choice of concrete mix, geometry of the samples and exposure conditions.

On the basis of the performance recorded from the investigations undertaken with different kinds of repair mortars and, in case, with an additional alkanolamine-inhibitor-based treatment for corroding reinforced concrete, it appears that it is important to rehabilitate deteriorated concrete structures using a good barrier effect coating. Thus, the repair mortar must have low porosity, low conductivity and low permeability to aggressive substances to prevent corrosion from chloride ingress in the cover. Moreover, it appears that inhibitor, when applied at the interface between concrete and repair grout, can cause some reduction in the corrosion rate of pre-corroding steel in concrete with high levels of chloride contamination.

The use of an alkanolamine-based migrating inhibitor as supplementary anticorrosion system appears to extend the rehabilitation and protection properties of a low-porosity repair mortar. When the inhibitor has been used in association with grouts which did not allow the ingress of aggressive solution from the external environment, the return to passivity was possible for the rebars which were initially corroded by the chlorides present in the concrete mix. The application of the inhibitor at the interface of the concrete substrate and the repair mortar can be considered very important. Probably the presence of a barrier layer with low permeability did not allow the volatile substances of the MCI to come out from the system.

In the case of repairs with high-porosity grouts, it was found that the inhibitor was effective under the condition studied only in retarding the onset of severe corrosion but did not show long-term effectiveness.

A possible inhibitor migrating effect can be deduced from the acceleration of the repassivation phenomena noted on the lower rebars of the specimens treated with the inhibitor. However, it cannot be stated for sure that inhibitor ions can be transported through realistic thickness of cover concrete of high w/c ratio, because repassivation occurred also in blank specimens.

Acknowledgements

Special thanks to Autobrennero S.p.a. and Tecnochem Italiana s.r.l. for the collaboration and the samples preparation. Besides, thanks to Alexia Conci for MIP measurements and to Luca Benedetti for chlorides analysis.

References

[1] G. Batis, P. Pantazopoulou, A. Routoulas, Corrosion protection investigation of reinforcement by inorganic coating in the presence of alkanolamine-based inhibitor, Cem. Concr. Compos. 25 (2003) 371–377.
[2] B. Elsener, Macrocell corrosion of steel in concrete—Implications for corrosion monitoring, Cem. Concr. Compos. 24 (2002) 65–72.
[3] G. Batis, A. Routoulas, E. Rakanta, Effects of migrating inhibitors on corrosion of reinforcing steel covered with repair mortar, Cem. Concr. Compos. 25 (2003) 109–115.
[4] C.M. Hansson, L. Mammoliti, B.B. Hope, Corrosion inhibitors in concrete: Part 1. The principles, Cem. Concr. Res. 28 (12) (1998) 1775–1781.
[5] B. Elsener, M. Buechler, F. Stalger, H. Boehni, Migrating corrosion inhibitor blend for reinforced concrete: Part 2. Inhibitor as repair strategy, Corrosion 56 (7) (2000) 52–56.
[6] B. Bavarian, L. Reiner, Migrating corrosion inhibitor protection of steel rebar in concrete, Mater. Perform. (NACE) 2 (2003) 3–5.
[7] F. Moro, H. Bohni, Ink-bottle effect in mercury intrusion porosimetry of cement-based materials, J. Colloid Interface Sci. 246 (2002) 135–149.
[8] L. Dhouibi, E. Triki, A. Raharinaivo, The application of electrochemical impedance spectroscopy to determine the long-term effectiveness of corrosion inhibitors for steel in concrete, Cem. Concr. Compos. 24 (2002) 35–43.

[9] A.B. Abell, K.L. Willis, D.A. Lange, Mercury intrusion porosimetry and image analysis of cement-based materials, J. Colloid Interface Sci. 211 (1999) 39–44.
[10] R.A. Cook, K.C. Hover, Mercury intrusion porosimetry of hardened cement pastes, Cem. Concr. Res. 29 (1999) 933–943.
[11] S. Diamond, Mercury porosimetry—An inappropriate method for the measurement of pore size distributions in cement-based materials, Cem. Concr. Res. 30 (2000) 1517–1525.
[12] E. Bottari, A. Liberti, Analisi chimica quantitativa, Università degli studi di Roma, Napoli-Fototipolitografia SO.GRA.ME.
[13] C. Andrade, C. Alonso, Corrosion rate monitoring in the laboratory and on-site, Constr. Build. Mater. 10 (5) (1996) 315–328.
[14] European concerted action COST 509, Final Report, Corrosion and protection of metals in contact with concrete: Part 2. Monitoring, European Commission, Brussel, February 1997, p.73.
[15] A.M. Vaysburd, P.H. Emmons, How to make today's repair durable for tomorrow—Corrosion protection of concrete repair, Constr. Build. Mater. 14 (2000) 189–197.